Penerbit Akademia Baru

Progress in Energy and Environment

Journal homepage: http://www.akademiabaru.com/progee.html
ISSN: 2600-7762

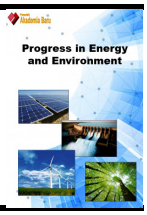


# Power Loss in Straight Polygon Pipe via CFD Simulation

Open Access

Wah Yen Tey*[,1,2], Hooi Siang Kang[3]

[1] Department of Mechanical Engineering, Faculty of Engineering, UCSI University, Kuala Lumpur, Malaysia
[2] Malaysia-Japan International Institute of Technology, Universiti Teknologi Malaysia, Kuala Lumpur, Malaysia
[3] Marine Technology Centre, Universiti Teknologi Malaysia, 81310 UTM Skudai, Johor, Malaysia

**ARTICLE INFO**

***Article history:***
Received 18 October 2018
Received in revised form 7 November 2018
Accepted 7 November 2018
Available online 9 November 2018

**ABSTRACT**

In most of the investigations on energy loss and friction factor of internal flow, circular tube is applied due to their wide availability and practicality. However, in some advanced engineering applications such as miniaturization of electrical devices, micro-scale heat pipes and medical tubes, the polygonal cross-sectional tube is often deployed. To investigate the flow energy requirement and flow characteristics of polygonal pipe, numerical simulation assisted by CFD commercial software ANSYS Fluent has been conducted. Stress-Strain Transport $k$-$\omega$ model has been applied to resolve the sensitivity of non-slip wall. In our simulation, we have considered water flow across the pentagon, hexagon and heptagon at turbulent region of Re from $5\times10^5$ to $5\times10^6$. Our simulation found that power lost will increase with respect to smaller number of polygonal edges. At low Reynolds number, the power loss will be generally higher too.

***Keywords:***
Polygon pipe, Power lost, Pressure drop, Polygon velocity profile, SST k-omega



## 1. Introduction

Analysis of the pressure drop and energy lost for internal flow has been studied extensively [1-4] for various engineering applications such as petrol-chemical transport [5], automobile fluid transport [6], water distribution network [7] and the development of heat pipe [8,9]. An understanding for internal flow field is important for prediction of pumping power requirement and design of energy-saving piping network. Some previous research works in internal flow are summarised here. Hwang and Kim [10], Zhigang et al. [11], Barlak et al. [12] and Hong et al. [13] investigated heat transfer, friction factor and pressure drop in microtube. The flow physics in spiral tube for heat transfer enhancement were reported by Ghodabi and Muzychka [14], Jalaludin and Miyara [15] and Li et al. [16]. Magnetohydrodynamic (MHD) interactions of internal flow can be referred to the works by Nakamura et al. [17] and Buhler and Mistrangelo [18]. The flow-structure interaction due to different fluids in the pipe such as non-Newtonian fluids [19,20], nanofluids [21-23] and multiphase fluids [24,25] is widely studied as well. Most of the pipe used in the abovementioned engineering application is in circular shape, due to its excellent ability to deal with external loads and feasibility for installation.

*Corresponding author.
*E-mail address: teywy@ucsiuniversity.edu.my*

However, there are some modern applications which deploy polygonal pipes, due to their geometrical congruency to the environmental requirement (i.e. packed on flat surface) [26]. For instance, the analysis of duct conductance in vacuum science and space engineering [27,28] and miniaturisation of electronic devices i.e. micro-heat pump design [29,30] are requiring polygonal tubes. A good design of polygonal pipe is beneficial for improving energy efficiency in flow suction and ventilation [31,32]. Unfortunately, the investigation of the flow dynamics in such a pipe is scarce.

With this regard, the objective of the paper is to investigate the friction factor, power loss and developed cross-sectional velocity contour of pentagon (five-edge pipe), hexagon (six-edge pipe) and heptagon (seven-edge pipe). The flow fields will be investigated at turbulent flow region. *k-ω* SST model [33] is applied with the assistance of CFD commercial software ANSYS Fluent.

## 2. Parameters used in the Study

The schematic drawing of polygon shape of pentagon (five-edge pipe), hexagon (six-edge pipe) and heptagon (seven-edge pipe) can be illustrated as in Fig. 1. The length of the edge, $x$ is pre-defined to be 20 cm, while the length of pipe, $L$ is set as 200 cm.

The Reynolds number (Re) of these pipes can be calculated as in Eq. (1):

$$\mathrm{Re} = \frac{\rho v D_h}{\mu} \tag{1}$$

in which $\rho$, $v$, $D_h$ and $\mu$ are fluid density, incoming flow velocity, hydraulic diameter and dynamic viscosity respectively. Meanwhile the hydraulic diameter of pentagon, hexagon and heptagon can be obtained via Eqs. (2.1) – (2.3) respectively. The details of the derivation of hydraulic diameter can be found in many fluid mechanics references [34,35].

$$D_{h,\mathrm{pentagon}} = \frac{x}{5}\sqrt{5\left(5+2\sqrt{5}\right)} \tag{2.1}$$

$$D_{h,\mathrm{hexagon}} = \sqrt{3}x \tag{2.2}$$

$$D_{h,\mathrm{heptagon}} = \cot\left(\frac{180}{7}\right)x \tag{2.3}$$

In our simulation, $x$ is taken as 20 cm. The density ($\rho$), specific heat ($C_P$), thermal conductivity ($k$) and dynamic viscosity ($\mu$) of the fluid are 998.2 kg/m$^3$, 0.6 J/kg·K, 4185.5 W/m·K and 0.001013 kg/ms respectively. The inlet velocity for the polygon pipe, which corresponds to Re from $5\times10^4$ to $5\times10^5$ can be tabulated as in Table 1 upon calculation from Eqs. (1) – (2.3). The inlet flow velocity is in uniform shape, and entry length will be required prior to the formation of steady and fully developed flow. Moreover, all the walls are set to be isothermal and no-slipping with roughness constant of 0.5.

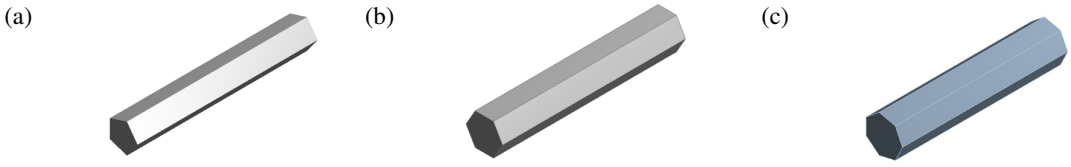


**Fig. 1.** Three-dimensional schematic drawing of polygonal pipe for (a) pentagon shape; (b) hexagon shape; and (c) heptagon shape

**Table 1** Velocity inlet (m/s) of the straight polygon pipe due to different Reynolds number

| Re | Pentagon | Hexagon | Heptagon |
|---|---|---|---|
| $0.5\times10^5$ | 0.1843 | 0.1465 | 0.1222 |
| $1.0\times10^5$ | 0.3687 | 0.2930 | 0.2445 |
| $1.5\times10^5$ | 0.5530 | 0.4394 | 0.3667 |
| $2.0\times10^5$ | 0.7373 | 0.5859 | 0.4889 |
| $2.5\times10^5$ | 0.9216 | 0.7324 | 0.6112 |
| $3.0\times10^5$ | 1.1060 | 0.8789 | 0.7334 |
| $3.5\times10^5$ | 1.2903 | 1.0253 | 0.8556 |
| $4.0\times10^5$ | 1.4746 | 1.1718 | 0.9779 |
| $4.5\times10^5$ | 1.6590 | 1.3183 | 1.1001 |
| $5.0\times10^5$ | 1.8433 | 1.4648 | 1.2224 |

The friction factor of the polygonal pipe, $f$ will be deduced via Eq. (3) and compared with the friction factor caused by a circular pipe with equivalent hydraulic radius. Meanwhile the power waste of the pipe, $W$ can be obtained from Eq. (4).

$$f = \Delta P \frac{D}{L}\frac{2}{\rho v^2} \tag{3}$$

$$W = \Delta P \frac{v\pi {D_h}^2}{4} \tag{4}$$

where $\Delta P$ refers to the pressure loss in the pipe.

## 3. Numerical Modelling

The governing equations applied are the Reynolds-averaged Continuity and Reynolds-averaged Navier-Stokes Equations (RANS), in which their simplified form can be shown in Eq. (5.1) and (5.2) respectively. RANS scheme has been widely applied for solving turbulent flow problem [36]. In current work, the scope is limited to incompressible flow and Newtonian fluid. No body force is exerted on the structure of polygonal pipes.

$$\nabla.\bar{\mathbf{u}} = 0 \tag{5.1}$$

$$\bar{\mathbf{u}}.\nabla\bar{\mathbf{u}} = -\nabla\bar{P} + \mu\nabla^2\bar{\mathbf{u}} \tag{5.2}$$

where $\nabla$ is divergent operator, $\bar{\mathbf{u}}$ is Reynolds-averaged velocity field and $\bar{P}$ is Reynolds-averaged pressure field respectively. The Reynolds-averaged fields are indeed the combination between the averaged value and its residuals, leading to additional four unknowns which cannot be solved only using Eq. (6.1) and (6.2). To fitting the missing equations, the two-equations Stress-Strain Transport (SST) $k$-$\omega$ model [33,37,38] has applied. SST scheme is proven to be able to resolve the near-wall viscous sublayer without incurring over-sensitivity at the far-field region [39-41]. The equations of turbulent kinetic energy ($k$-equation) and specific dissipation rate equation ($\omega$-equation) can be described as in Eq. (6.1) and (6.2) respectively:

$$\nabla\left(\rho k\bar{\mathbf{u}}\right) = \nabla\left(\mu_{eff,k}\nabla k\right) + \tilde{P}_k - \rho\beta k\omega \tag{6.1}$$

$$\nabla\left(\rho\omega\bar{\mathbf{u}}\right) = \nabla\left(\mu_{eff,\omega}\nabla k\right) + \alpha {v_t}^{-1}\tilde{P}_k - \rho\beta\omega^2 + 2\left(1-F\right)\rho\sigma_{\omega,2}\omega^{-1}\left(\nabla k\right)\left(\nabla\omega\right) \tag{6.2}$$

in which $\mu_{eff,k}$ is the effective diffusivities for turbulent kinetic energy, $\mu_{eff,\omega}$ is the effective diffusivities for specific dissipation rate, $\beta$ is an applied constant, $\tilde{P}_k$ is the production limiter to prevent turbulence build-up in stagnation region, $\alpha$ is a function relating specific dissipation rate with production limiter and $F$ is the blending functions respectively. The detailed formulation of SST models can be found in [33,37,38,42,43].

For pressure-velocity coupling scheme, the Semi-Implicit Method for Pressure-Linked Equations (SIMPLE) algorithm as proposed by Patankar and Spalding [44] is applied. SIMPLE algorithm works

based on the continuous guess-and-correction principle for both velocity and pressure field, fulfilling the continuity and momentum principle as outlined in Eq. (3.1) and (3.2). In the mathematical formulation of SIMPLE scheme, under-relaxation factor plays an important role to prevent numerical fluctuation and divergence [45]. In the current work, the under-relaxation factor set for the pressure, momentum, $k$ and $\omega$ is 0.25, 0.7, 0.8 and 0.8 respectively. Second order upwind discretisation method is applied for the convection term while first order upwind is applied for $k$ and $\omega$. The convergence criteria for all continuity, momentum, $k$ and $\omega$ are set at a very low value of $10^{-6}$ to minimise the numerical error. However, in our simulation, even with extended iterations, the continuity residual keeps floating at about $10^{-5}$, possibly due to the pressure fluctuation at the corner of the edges.

The tetrahedron patch-conforming meshing is used with improved mesh treatment at the no-slip walls, as shown in Fig. 2. The maximum layer at the boundary is set as 20. Upon the mesh independence studies as in Table 2, the element size used for the simulation is 1.6 cm. The value of pressure drop is of little difference even the element size is further reduced.

**Table 2** Pressure drop (kPa) of the polygon pipes at Re = $5\times10^5$ for mesh independence study

| Element Size | Pentagon | Hexagon | Heptagon |
|---|---|---|---|
| 1.7 cm | 0.2278 | 0.1214 | 0.07423 |
| 1.6 cm | 0.2283 | 0.1215 | 0.07412 |
| 1.5 cm | 0.2279 | 0.1215 | 0.07411 |
| 1.4 cm | 0.2281 | 0.1217 | 0.07455 |

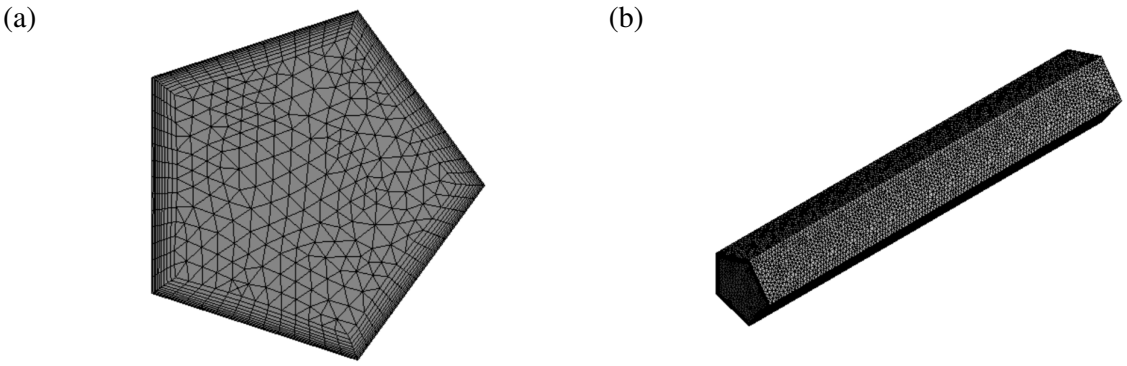


**Fig. 2.** Tetrahedron patch-conforming meshing applied for the pentagonal pipe at (a) cross-sectional view; and (b) isometric view.

## 4. Results and Discussion

From the results of the simulation from Figs. 3-5, all the polygonal pipes generally will have larger friction factor compared with their respective circular pipe with equivalent hydraulic diameter. The friction factor decreases exponentially with respect to the increment of Reynolds number. At highly turbulent region the increment of value of friction factor becomes smaller, and this trendline is in accordance with the Colebrook-White correlation as in Eq. (7), which can be clearly represented in Moody chart.

$$\frac{1}{f} = -2.0\log\left(\frac{\varepsilon / D_h}{3.71} + \frac{2.51}{\mathrm{Re}\sqrt{f}}\right) \tag{7}$$

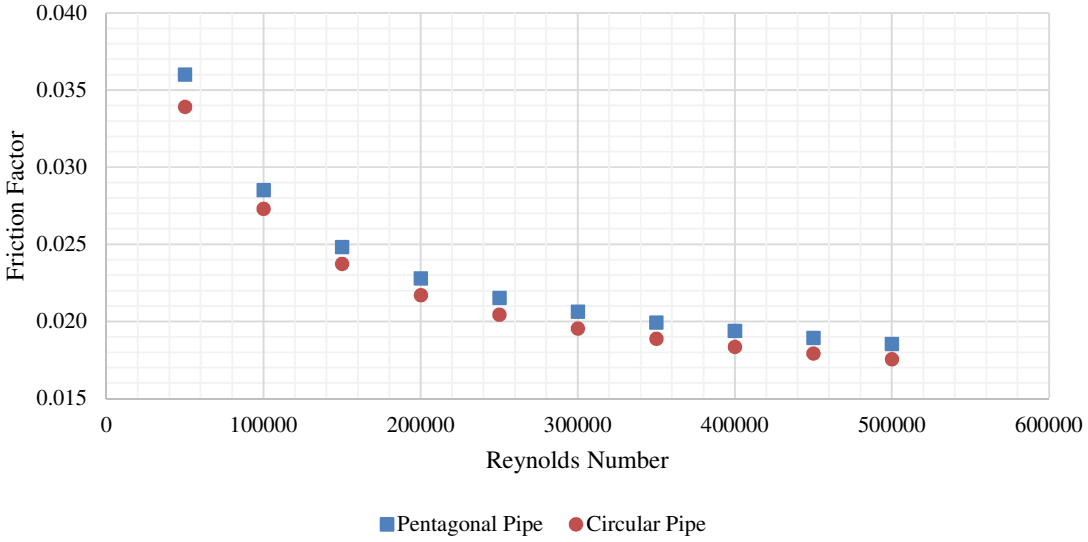


**Fig. 3.** Friction factor for pentagonal pipe and its equivalent circular pipe at different Reynolds number

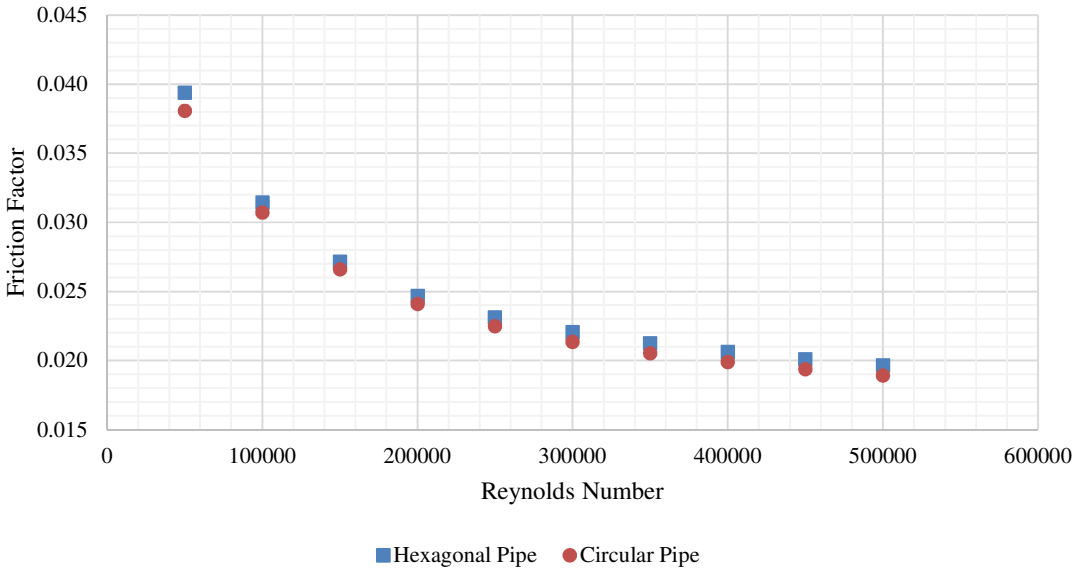


**Fig. 4.** Friction factor for hexagonal pipe and its equivalent circular pipe at different Reynolds number

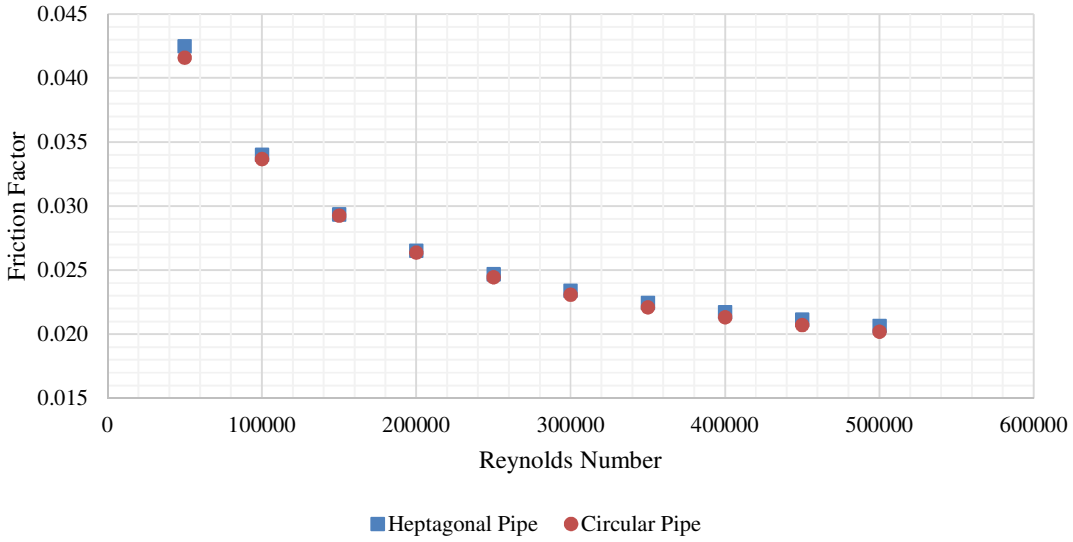


**Fig. 5.** Friction factor for heptagonal pipe and its equivalent circular pipe at different Reynolds number

It is noteworthy that at low Reynolds number, the difference of friction factor between the polygonal pipes and circular pipes is large. However, when the flow goes more turbulent, the friction factor between them starts to converge. This can be ascribable to the overwhelming momentum effect of the flow, negating the wall friction [35].

Amongst the investigated pipe, pentagonal pipe suffers the highest friction factor and power loss increment compared with its equivalent circular pipe, as shown in Figs. 6 and 7 respectively. The friction factor and power loss increment can be calculated from Eqs. (8) and (9) respectively. It can be observed that when the number of edges increases, the friction factor and power loss increment will drop too. When the number of edges reaches to an amount which makes cross-sectional geometry resembling a circle, there will be of very little difference with the circular pipe.

$$\Delta f = \frac{f_{polygon} - f_{circular}}{f_{circular}} \times 100\% \tag{8}$$

$$\Delta W = \frac{W_{polygon} - W_{circular}}{W_{circular}} \times 100\% \tag{9}$$

For both $\Delta f$ and $\Delta W$, with the increment of the Reynolds number, they will drop to a minimum point before their steady increment, most probably due to the reason that the flow may still in laminar or transitional region. At high Reynolds number, the $\Delta f$ and $\Delta W$ will gradually goes stable too. The Reynolds-averaged friction factor increment for pentagonal, hexagonal and heptagonal pipe is 5.35%, 3.11% and 1.42% respectively. The exact correlation between the friction factor increment and Reynolds number for pentagonal, hexagonal and heptagonal pipe can be computed as in Eqs. (10.1) – (10.3) respectively:

$$\Delta f = -5\times10^{-27}\,\mathrm{Re}^5 + 8\times10^{-21}\,\mathrm{Re}^4 - 5\times10^{-15}\,\mathrm{Re}^3 + 1\times10^{-9}\,\mathrm{Re}^2 - 2\times10^{-4}\,\mathrm{Re} + 11.471 \tag{10.1}$$

$$\Delta f = -1\times10^{-27}\,\mathrm{Re}^5 + 2\times10^{-21}\,\mathrm{Re}^4 - 2\times10^{-15}\,\mathrm{Re}^3 + 6\times10^{-10}\,\mathrm{Re}^2 - 9\times10^{-5}\,\mathrm{Re} + 6.4578 \tag{10.2}$$

$$\Delta f = -3\times10^{-28}\,\mathrm{Re}^5 + 2\times10^{-22}\,\mathrm{Re}^4 - 6\times10^{-16}\,\mathrm{Re}^3 + 4\times10^{-10}\,\mathrm{Re}^2 - 7\times10^{-5}\,\mathrm{Re} + 4.8903 \tag{10.3}$$

where the coefficient of determination ($R^2$) is 0.9869, 0.9972 and 0.9947 respectively. The large friction factor at the pentagon can be caused by the large eddy viscosity formed around the wall as shown in Fig. 8, which further calls for larger pumping power to push the flow. The eddy viscosity

will alter the velocity profile in a way that: Stoke's flow happens at the near-wall region while Hagen-Poiseuilli flow happens at the middle of the pipe.

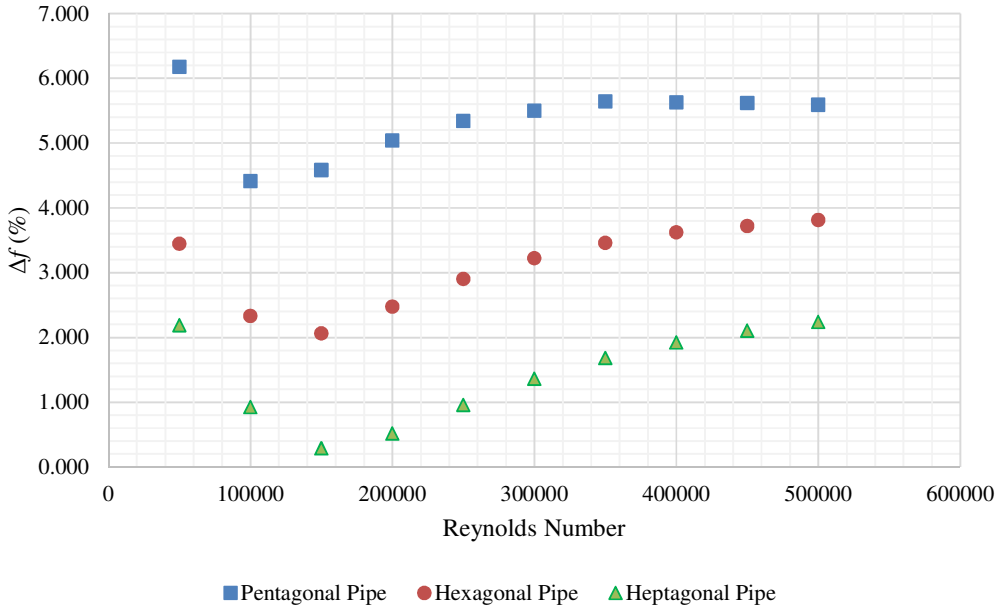


**Fig. 6.** Friction factor increment for polygonal pipes in comparison with its equivalent circular pipe at different Reynolds number

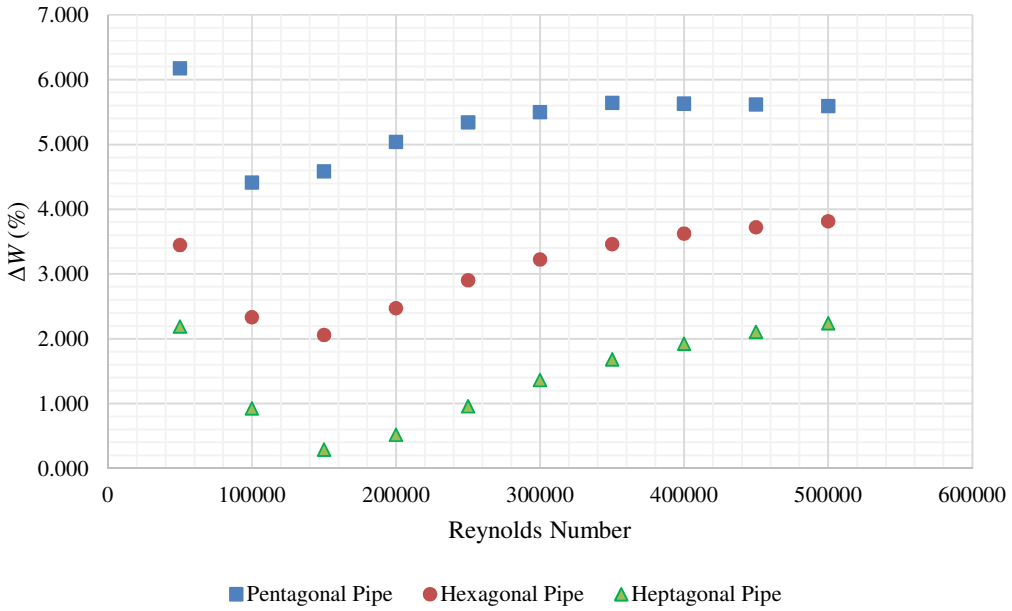


**Fig. 7.** Power loss increment for polygonal pipes in comparison with its equivalent circular pipe at different Reynolds number

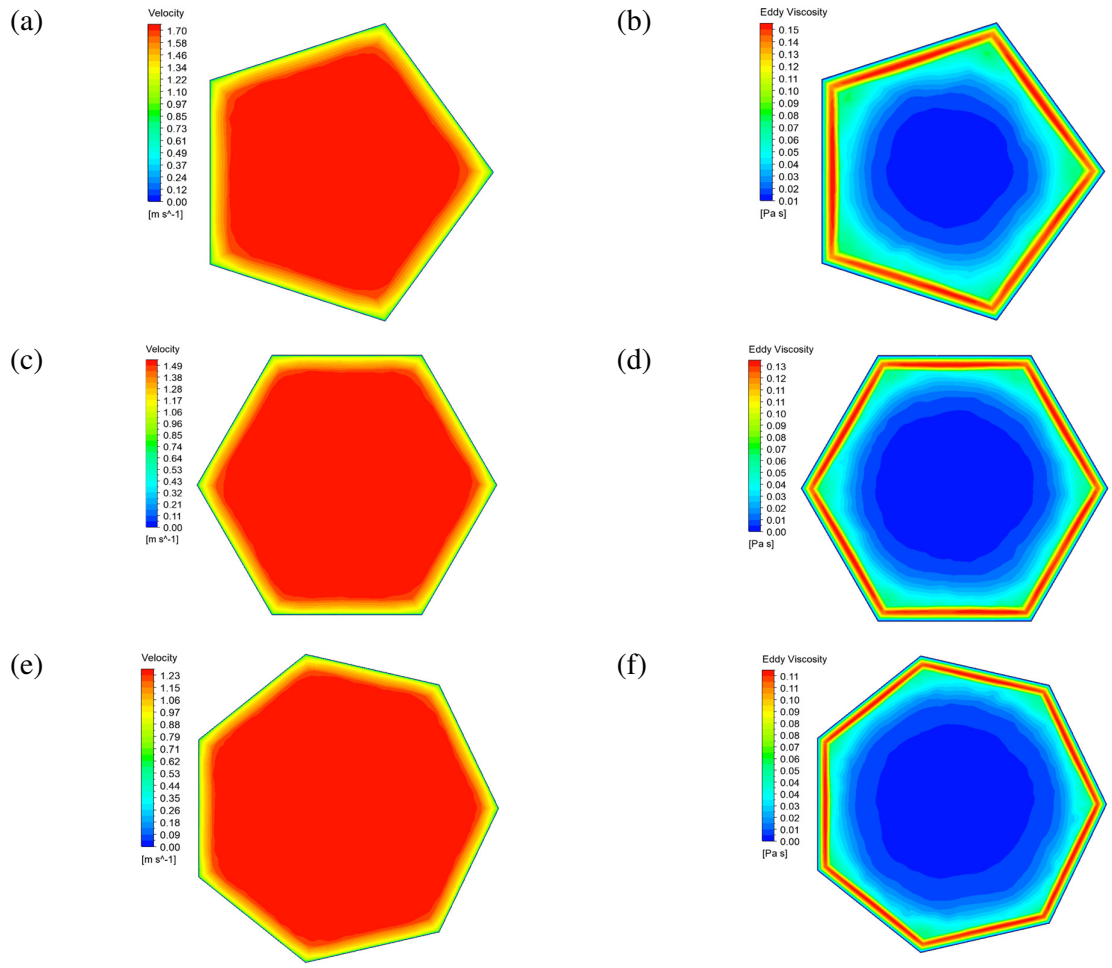


**Fig. 8.** The cross-sectional plot for: (a) velocity contour of pentagonal pipe; (b) eddy viscosity contour of pentagonal pipe; (c) velocity contour of hexagonal pipe; (d) eddy viscosity contour of hexagonal pipe; (e) velocity contour of heptagonal pipe; (f) eddy viscosity contour of heptagonal pipe; when Re = $5.0\times10^5$

## 5. Conclusion

In conclusion, pentagonal pipe will result in the highest loss of power, followed by hexagonal and heptagonal pipe in the analysis. The conventional Colebrook-White Equation is proven unsuitable for application of polygonal pipes, as the friction factor is generally higher for all polygonal pipes. The correlation between the friction factor increment and Reynolds number has been computed for all the polygonal pipes as well for further investigation and future application.

## References

[1] Chen, J., Cui, G.X., Xu, C.X., Zhang, Z.S. and Nieuwstadt, F.T.M. "Numerical study of transition in a cylindrical pipe flow." *Communications in Nonlinear Science and Numerical Simulation* 9(6) (2004): 661-668.

[2] Tey, W.Y., Tan, L.K. and Ang, C.K. "A Highly Computationally Efficient Explicit-Iterative Hybrid Algorithm for Colebrook-White Equation." In *7th International Conference on Software and Computer Applications*, pp. 269-273, 2018.

[3] Wang, Z., Orlu, R., Schlatter, P. and Chung, Y.M. "Direct numerical simulation of a turbulent 90° bend pipe flow." *International Journal of Heat and Fluid Flow* 73 (2018): 199-208.

[4] Peng, C., Geneva, N., Guo, Z. and Wang, L.P. "Direct numerical simulation of turbulent pipe flow using the lattice Boltzmann method." *Journal of Computational Physics* 357 (2018): 16-42.

[5] Bursi, O., Reza, M.S., Abbiati, G. and Paolacci, F. "Performance-based earthquake evaluation of a full-scale petrochemical piping system." *Journal of Loss Prevention in the Process Industries* 33 (2015): 10-22.
[6] Fomenko, N.A., Aleksikov, S.V. and Artyomova, S.G. "High pressure piping of tractive transport vehicles." *Procedia Engineering* 150 (2016): 1359-1362.
[7] Hajibabaei, M., Nazif, S., Sereshgi, F.T. "Life cycle assessment of pipes and piping process in drinking water distribution networks to reduce environmental impact." *Sustainable Cities and Society* 43 (2018): 538-549.
[8] Zhao, X.X., Fu, H., Ji, J., Sun, H., Ma, R. and Wu, X. "Comparative study on performances of a heat-pipe PV/T system and a heat-pipe solar water heating system." International Journal of Green Energy 13 (2016): 229-240.
[9] Bastakoti, D., Zhang, H., Li, D., Cai, W. and Li, F. "An overview on the developing trend of pulsating heat pipe and its performance." *Applied Thermal Engineering* 141 (2018): 305-332.
[10] Hwang, Y.W. and Kim, M.S. "The pressure drop in microtubes and the correlation development." *International Journal of Heat and Mass Transfer* 49 (11) (2006): 1804-1812.
[11] Zhigang, L., Ning, G., Chengwu, Z. and Xiaobao, Z. "Experimental study on flow and heat transfer in a 19.6-μm microtube." *Experimental Heat Transfer* 22 (3) (2009): 178-197.
[12] Barlak, S., Yapici, S. and Sara, O.N. "Experimental investigation of pressure drop and friction factor for water flow in microtubes." *International Journal of Thermal Sciences* 50 (3) (2011): 361-368.
[13] Hong, C., Tanaka, G., Asako, Y. and Katanado, H. "Flow characteristics of gaseous flow through a microtube discharged into the atmosphere." *International Journal of Heat and Mass Transfer* 121 (2018): 187-195.
[14] Ghodabi, M. and Muzychaka, Y.S. "Heat transfer and pressure drop in a spiral square channel." *Experimental Heat Transfer* 28 (6) (2015): 546-563.
[15] Jalaluddin and Miyara, A. "Thermal performance and pressure drop of spiral-tube ground heat exchangers for ground-source heat pump." *Applied Thermal Engineering* 90 (2015): 630-637.
[16] Li, S., Cai, W., Chen, J., Zhang, H. and Jiang, Y. "Numerical study on the flow and heat transfer characteristics of forced convective condensation with propane in a spiral pipe." *International Journal of Heat and Mass Transfer* 117 (2018): 1169-1187.
[17] Nakamura, S., Kunugi, T., Yokomine, T., Kawara, Z., Kusumi, K., Sagara, A., Yagi, J. and Tanaka, T. "MHD pressure drop measurement of PbLi flow in double-bended pipe." *Fusion Engineering and Design* (2017): In corrected proof.
[18] Buhler, L. and Mistrangelo, C. "Pressure drop and velocity changes in MHD pipe flows due to a local interruption of the insulation." *Fusion Engineering and Design* 127 (2018): 185-191.
[19] Cho, Y.I. and Harnett, J.P. "Non-Newtonian fluids in circular pipe flow." *Advances in Heat Transfer* 15 (1982): 59-141.
[20] Pinho, F.T. and Whitelaw, J.H. "Flow of non-newtonian fluids in a pipe." *Journal of Non-Newtonian Fluid Mechanics* 34 (2) (1990): 129-144.
[21] Hassan, M.I., Alzarooni, I.A. and Shatilla, Y. "Heat pipe long term performance using water based nanofluid." *Cogent Engineering* 4 (1) (2017): Article: 1336070.
[22] Yin, Z., Bao, F., Tu, C., Hua, Y. and Tian, R. "Numerical and experimental studies of heat and flow characteristics in a laminar pipe flow of nanofluid." *Journal of Experimental Nanoscience* 13 (1) (2018): 82-94.
[23] Minea, A.A. and Estelle, P. "Numerical study on CNT nanofluids behavior in laminar pipe flow." *Journal of Molecular Liquids* 217 (2018): 281-289.
[24] Duan, J. and Zhou, J. "Studies on frictional pressure drop of gas-non-Newtonian fluid two-phase flow in the vacuum sewers." *Civil Engineering and Environmental Systems* 23 (1) (2006): 1-10.
[25] Kong, R., Kim, S., Bojerek, S., Tian, K. and Hoxie, C. "Effects of pipe size on horizontal two-phase flow: Flow regimes, pressure drop, two-phase flow parameters, and drift-flux analysis." *Experimental Thermal and Fluid Science* 96 (2018): 75-89.
[26] Li, Y., Chen, X., Wang, L., Guo, L. and Li, Y. "Molecular flow transmission probabilities of any regular polygon tubes." *Vacuum* 92 (2013): 81-84.
[27] Gómez-Goñi, J. "Comparison between Monte Carlo and analytical calculation of the conductance of cylindrical and conical tubes." *Journal of Vacuum Science & Technology A* 21 (2003): 1452.
[28] Li, Y., Chen, X., Li, D., Xiao, Y., Dai, P. and Gong, C. "Design and analysis of vacuum air-intake device used in air-breathing electric propulsion." *Vacuum* 120 (2015): 89-95.
[29] Moon, S.H., Hwang, G., Ko, S.C. and Kim, Y.T. "Experimental study on the thermal performance of micro-heat pipe with cross-section of polygon." *Microelectronics Reliability* 44 (2) (2004): 315-321.
[30] Suman, B. and Kumar, P. "An analytical model for fluid flow and heat transfer in a micro-heat pipe of polygonal shape." *International Journal of Heat and Mass Transfer* 48 (21-22) (2005): 4498-4509.
[31] Wong, K.L., Chou, H.M. and Li, Y.H. "Complete heat transfer solutions of an insulated regular polygonal pipe by using a PWTR model." *Energy Conversion and Management* 45 (11-12) (2004): 1705-1724.
[32] Lv, W., Shen, C. and Li, X. "Energy efficiency of an air conditioning system coupled with a pipe-embedded wall and mechanical ventilation." *Journal of Building Engineering* 15 (2018): 229-325.
[33] Menter, F.R. "Two-equation eddy-viscosity turbulence models for engineering applications." *AIAA Journal* 32

(1994): 1598-1605.
[34] Munson, B.R., Young, D.F. and Okiishi, T.H. Fundamentals of Fluid Mechanics. John Wiley and Sons, 2006.
[35] Cengel, Y. and Cimbala, J. Fluid Mechanics: Fundamentals and Applications. McGraw Hill Education, 2014.
[36] Tey, W.Y., Asako, Y., Sidik, N.A.C. and Goh, R.Z. "Governing equations in computational fluid dynamics: Derivations and a recent review." *Progress in Energy and Environment* 1 (2017): 1-19.
[37] Menter, F.R. "Zonal two equation kappa-omega turbulence models for aerodynamic flows." In: *24th AIAA Fluid Dynamics Conference*, Orlando, Florida, USA, 1993.
[38] Menter, F.R. "Review of Shear-Stress Transport turbulence model experience from an industrial perspective." *International Journal of Computational Fluid Dynamics* 23 (2009): 305-316.
[39] Ugur, O.U., Mehmet A. and Omer, G. "Effect of turbulence modelling on the computation of near-wake flow of a circular cylinder." *Oceanic Engineering* 37 (2010): 387-399.
[40] Jubayer, C.M. and Hangan, H. "Numerical simulation of wind effects on a stand-alone ground mounted photovoltaic (PV) system." *Journal of Wind Engineering and Industrial Aerodynamics* 134 (2014): 56-64.
[41] Sidik, N.A.C. and Tey, W.Y. "Reynolds number – Strouhal number relationship for cylindrical bluff body with variation of aspect ratio in high Reynolds number." *Jurnal Teknologi* 69 (3) (2014): 125-128.
[42] Rocha, P.A.C., Rocha, H.H.B., Carneiro, M., da Silva, M.E. and Bueno, V. "*k-ω* SST (shear stress transport) turbulence model calibration: A case study on a small scale horizontal axis wind turbine." *Energy* 65 (2014): 412-418.
[43] Yu, H. and The, J. "Validation and optimization of SST *k-ω* turbulence model for pollutant dispersion within a building array." *Atmospheric Environment* 145 (2016): 225-238.
[44] Patankar, S.V. and Spalding, D.B. "A calculation procedure for heat, mass and momentum transfer in three-dimensional parabolic flows." *International Journal of Heat and Mass Transfer* 15 (1972): 1787.
[45] Lee, C.E., Tey, W.Y. and Tan, L.K. "The investigation on SIMPLE and SIMPLER algorithm through lid driven cavity." *Journal of Advanced Research in Fluid Mechanics and Thermal Sciences* 29 (1) (2017): 10-23.